Experimental Analysis on Thermal Characteristics of Argan Nut Shell (ANS) Biomass as a Green Energy Resource

Yassine Rahib*, **‡, Abdallah Elorf*, Brahim Sarh**, Sylvie Bonnamy***, Jamal Chaoufi**, Mohamed Ezahri****

* Institute of Combustion, Aerothermal, Reactivity and Environment, UPR 3021 of CNRS, Orleans University, Orleans, France

** Laboratory of Electronics, Signal Processing and Modelling Physics, Department of Physics, Ibn Zohr University, 80000 Agadir, Morocco

*** Laboratory of Confinement, Materials and Nanostructures, UMR 7374, CNRS, University of Orleans, 45071 Orleans Cedex 2, France

**** Laboratory of Materials and Environment, Faculty of Sciences, Ibn Zohr University, 80000 Agadir, Morocco

(yassine.rahib@univ-orleans.fr, abdallah.elorf@univ-orleans.fr, brahim.Sarh@cnrs-orleans.fr, sylvie.bonnamy@cnrs-orleans.fr, jchaoufi@gmail.com, m.ezahri@uiz.ac.ma)

‡ Corresponding Author; First Author, Orleans 45100, Tel: +33 6 17384237, yassine.rahib@univ-orleans.fr

Abstract- Argan nut shell (ANS) is one of the most abundant agricultural by-product in the southwestern of Morocco. This study aims to focus on thermal characteristics of ANS biomass for alternative energy production. Physicochemical studies were done to characterize biomass-based material. Moreover, thermal degradation characteristics and kinetic parameters were assessed under pyrolysis and oxidizing conditions by means of thermogravimetric methods. Fundamental tests involving particle combustion of ANS and coal were carried out, and a comparison was performed. The results exhibit a negligible amount of nitrogen and sulfur and a heating value of 20.63 MJ kg^{-1} compared to 24 MJ kg^{-1} for high grad coals. Furthermore, ANS follows the usual structural decomposition of lignocellulosique biomass, while coal reveal a discrete devolatilization zone. In addition, combustion tests show a significant burning period and high particle temperature. This experimental research is intended to provide a reference data of ANS biomass for energy recovery through combustion.

Keywords Biomass, argan nut shell, thermogravimetric analysis, decomposition kinetics, particle combustion.

1. Introduction

Renewable energy has considered as an efficient way to remedy the energy crisis and climate change problems [1–3]. Nowadays, the energy recovery of agricultural residues as a source of biomass has attracted increasing attention [4-6]. Indeed, crop residues that include all agricultural waste have various economic and environmental benefits [7].

Argan (Argania spinoza) is the archetypal tree which values the southwestern province of Moroccan territory with 74% of the global production share, and approximately more

than 20 million trees, covering an area of 800 000 ha [8]. The main wealth of this plant is its fruit. The argan nut shell (ANS) is the rigid shell that represents the most of the net weight of argan nut (~80%), and which keeps the almond. The ANS can be considered as an attractive source of biomass, since it is procurable in abundance and do not contend with food product. This biomass is commercially produced especially in southwestern Morocco because of its high energy content (higher heating value of 17.29 MJ kg^{-1}) which make it an excellent biofuel [9]. Their selling price (0.05 euro/kg) remains very low compared to that of coal (energy content > 24 MJ kg^{-1} for high grad coals). The predominant use of ANS

is traditional fuel for heating and cooking due to its ability to keep fire for a long time. The potential valorization of ANS will contribute to extend the market of biomass and biofuels and will also help to solve the energetic problems at the local, regional, national and maybe the international level.

Generally, the ANS are traditionally used in many sectors. Bouqbis et al. studied the physicochemical characteristics of a biochar produced from ANS in a pyrolytic furnace, to be used in soil enrichment and retention of nutrients and water [10]. ANS is also used for the preparation of active carbons by physical and chemical activation processes [11]. In addition, Essabir et al. has studied the physical, mechanical and thermal properties of polypropylene-based bio-composites materials reinforced with ANS [12]. Nevertheless, according to our knowledge there are very few published studies in the literature which evaluating the potential use of ANS as a renewable energy source. In particular, Rahib et al. examined the potential of ANS as an energy source. This study investigates the thermokinetic characteristics of ANS under combustion in order to evaluate the potential valorization into a green energy source. The authors have noted that ANS has a great potential to produce energy through combustion [13].

Thermogravimetric techniques have been widely used to investigate the thermal degradation behavior of agricultural biomass under different atmospheric conditions. For instance, Alhinai et al. investigated the thermochemical conversion of rice husk during respective pyrolysis and combustion for biochar production potentiality [14]. Moreover, El may et al. studied the thermal behavior under inert and oxidizing atmospheres by TGA of fives biomass from Tunisian dates cultivation in order to evaluate their utility for energy production [15]. In addition, Munir et al. have used thermal analysis techniques to study degradation, reactivities and kinetic parameters of biomass [16].

Concerning the study of particle combustion, many of researches have been performed. Marek and Swiatkowski experimentally studied the combustion process of a single coal particle in different gas mixtures [17]. The authors measured the ignition and surface temperature of the particle conjointly with illustrated different combustion steps. Similarly, Jones et al. proposed a method based on thermal analyzes (TGA-DTG and DTA) and single-particle combustion tests for assessing the relative risk rating for the ignition of biomass fuels [18]. Recently, Riaza et al. developed a single particle combustion apparatus to investigate and observe the differences between conversion behavior of white wood pellets and Cerrejón coals [19].

The main objective of this work is to investigate combustion and thermal behaviors of the ANS biomass which is continuously growing, in order to optimize and better understand its thermochemical conversion, being an alternative way to efficiently recycle the ANS waste. For this purpose, a characterization of ANS was done. Moreover, thermal behaviors were studied via thermogravimetric analysis, and kinetic parameters were evaluated. Finally, combustion characteristics of ANS were determined and compared with those of coal by means of thermogravimetric analyzer and single particle combustion device.

2. Experimental study

2.1. Materials

Figure 1 illustrates the ANS residual used throughout this work. Experimental characterizations require a preliminary preparation since the samples were collected in the natural state. Preparation of samples is done by separation of shells from the rest of the almond. Recovered shells are crushed and sieved (200µm), in order to remove the coarse elements.
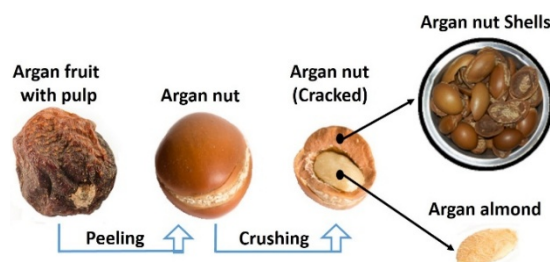

Fig. 1. Obtained ANS biomass after peeling the dried argan fruit and crushing the argan nut.

2.2. Physical characteristics

Density (ρ) is one of the physical properties that makes the use of biomass significant as a fuel especially in incineration industries where lightness is requested. Particle and powder densities of ANS were determined by immersion in water. Bulk density was also evaluated according to CEN TS15103 method [20] because of its great importance in terms of fuel logistics (storage, transport, and handling) and economical perspectives.

2.3. Fuel characteristics

2.3.1. Specific energy

The gross calorific value (GCV) of ANS was measured using a PARR 1261 calorimetric bomb. It gives information on the energy that can be extracted from the fuel. The net calorific value (NCV) and the energetic density were calculated [21].

2.3.2. Ultimate analysis

Ultimate analysis was carried out using an elementary analyzer CHONS-Thermo Scientific Flash 2000. Carbon, hydrogen, nitrogen and sulfur compositions were analyzed via flask combustion at 950 °C and the oxygen, gravimetrically, by pyrolysis at 1070 °C.

2.3.3. Proximate analysis

Proximate analysis consists in determining the moisture, volatile matter and ash content. It was carried out using a DTG-60 analyzer brand Shimadzu based on standard ASTM procedure. The fixed carbon content was estimated by difference [22]. In case of inert atmosphere, 30 min of N_2 purging was conducted for pushing the air and stabilizing the environment within the apparatus.

2.4. Thermogravimetric analysis

Thermogravimetric (TG) and differential thermal analysis (DTA) was carried out in dynamic conditions and the thermal behaviors of ANS biomass was evaluated in inert (N_2) and oxidative (air) atmospheres. TGA and DTA thermogram were obtained from room temperature to 600 °C at a heating rate of 10 °C min^{-1} and a gas flow rate of 20 ml min^{-1}. The derivative of thermogravimetric (DTG) was calculated. To ensure the precision thermogram, the DTG-60 was calibrated periodically with pure indium (99.99 %).

2.5. Experimental device and measurement technique

Figure 2 illustrates the experimental device which allows the particle combustion of ANS. Its consists of a vertical cylindrical combustion chamber made of sheet steel, with a height of 230 mm, a diameter of 190 mm and a 2 mm thick wall. An electrical heating resistance is placed at the bottom of the reactor for starting the combustion process. The particle is located in a steel grid placed 10 mm below the radiation heater. The combustion chamber is equipped with a thin K-type thermocouple placed at the center of the particle, and linked to a data logger for continuously recording the temperatures measured each second. A video camera installed in the horizontal plane of the grid allows having visual observations on ignition and combustion of the fuel. This set provides direct measurement and equitable information on igniting and burning processes of the ANS particle.
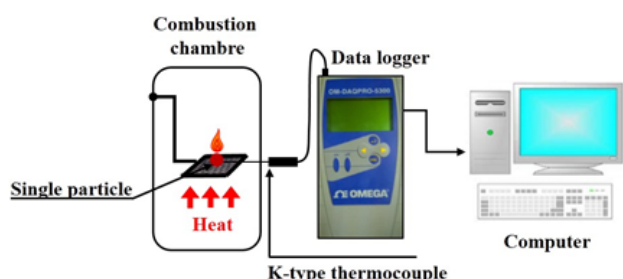

Fig. 2. Schematic diagram of the experimental facility for particle combustion.

3. Results and discussions

3.1. Argan nut shell characterization

To characterize ANS biomass, apparent density, calorific value, ultimate and proximate analyses was performed. The results of characterization are presented in Table 1. The considerable content of volatiles (67.5 %) is an attractive character that can improve the process of ignition during combustion. Ash content remains relatively low (1.5%) compared to other lignocellulosic biomasses [15, 16]. This would have contributed to reduce operational problems in the treatment, combustion and emissions. Moreover, the use of ANS as an alternative fuel to coal can significantly depress the costs associated with ash disposal. In addition, ANS has higher value of oxygen (42.35%) which reduces the energy content. The GCV and NCV for ANS was 20.63 and 17 MJ kg^{-1}, respectively. The empirical formula calculated from elemental composition is $C_{1.62}H_{2.39}O$. Moreover, molar ratios

H/C and O/C (on ash free dry basis) were determined as 1.48 and 0.62 respectively. The sulfur content is not detected, indicating that SO_x emissions will be negligible. Furthermore, the nitrogen percentage is very low (0.005 %), which could be a good character to reducing NO_x emissions during thermal conversion.

Table 1. Argan nut shell characteristics.

Characteristics	ANS sample
Densities [a] [Kg / m^3]	
Particle density	1060
Bulk density	596
Energy content	
GCV [a] [MJ / Kg; a.r.b.]	18.30
GCV calculated [MJ / Kg; d.b.]	20.63
NCV calculated [MJ / Kg; w.b.]	17
Energetic density [GJ / m^3]	10.13
Ultimate analysis [a, b] (wet. % w.b.)	
C	51.33
H	6.32
N	0.005
S	0
O	42.345
H / C molar ratio [b]	1.48
O / C molar ratio [b]	0.62
Empirical formula [b]	$C_{1.62}H_{2.39}O$
Proximate analysis (wet. %. a.r.b)	
Moisture	9.5
Volatile matter	67.5
Fixed carbon	21.5
Ash	1.5

[a] the essay was conducted in triplicated and the mean value is reported;
[b] measured on dry ash free basis.
Abbreviations: GCV= gross calorific value; NCV= net calorific value;
a.r.b. =as received basis; d.b. =dry basis; w.b. = wet basis.

3.2. Thermal behavior under inert atmosphere

In order to better understand the thermal degradation characteristics of ANS, and by reasoning that such variations in biomass degradation should be due to differences in elemental and chemical compositions of the samples, it worthwhile to consider the data of Essabir which indicate that ANS consists in three major components that are hemicellulose (24.3%), cellulose (40.7%) and lignin (32.5%) [23]. Moreover, those of Elabed indicate that the optimum temperature range for thermal decomposition of hemicellulose, cellulose and lignin are 280, 320 and 400 °C respectively [24]. By analogy, these results would help in our approach to explain the thermal decomposition mechanism.

The pyrolytic process of ANS is characterized by a mass loss made up of three stages (Fig. 3). The initial mass loss (9.5 %) occurring between 20 and 120 °C is attributed to the release of moisture from the particles. The second step (mass loss of 34.5%) is observed in the temperature range 231-328

°C, which corresponds to the thermal degradation of the hemicellulose. The third stage, in the temperature range 328-415 °C corresponds to the degradation of the cellulose component present in the particle, with a mass loss of 26%. The degradation of hemicellulose and cellulose leads to the release of volatile matter, which in turn leads to char formation (22.6%). The ANS exhibited a period of thermal stabilization in the range of 113-206 °C before particle ignition, making it a stable material during its storage as fuel.
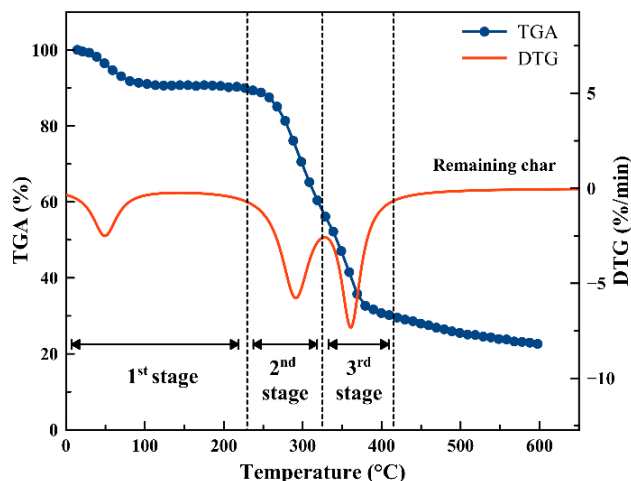

Fig. 3. TG-DTG curves under pyrolysis condition.

The DTG curve behaves as an indication of the ANS reactivity R_M (% min^{-1} $°C^{-1}$) [15, 16] which assumed directly proportionally to the maximum weight loss rate DTG_{max} (% min^{-1}) and inversely proportional to its corresponding temperature T_{DTGmax} (°C):

$$R_M = 100 * \sum \frac{\|DTG_{max}\|}{T_{DTG_{max}}} \qquad (1)$$

The R_M index reflects the measure of the decomposition rate of biomass structural components indicated by the DTG peak. The TG-DTG thermograms obtained under nitrogen atmosphere was analyzed to determine the pyrolysis parameters that have been listed in Table 2.

Table 2. TG-DTG characteristics of ANS under pyrolysis conditions (N_2) and comparison with other biomass residues.

TG-DTG characteristics	Stages	ANS	Cotton stalk	SCB
Reference		This work	[16]	[16]
Moisture	I	9.71	4	12
Temperature range (°C)	II III	231-328 328-415	200-425	214-424
T_{DTGmax}	II III	287 361	334	346
$\|DTG_{max}\|$	II III	5.6 7.2	10.8	10.2
$R_M * 10_2$	-	3.95	3.24	2.95
Residue	-	22.5	23	25

SCB: sugar cane bagasse, R_M: reactivity (% min^{-1} $°C^{-1}$)

ANS reactivity during pyrolysis proves its importance compared to other lignocellulosic biomasses [16]. This may be due to the fact that the early stage of decomposition of the hemicellulose (stage II) takes place at a temperature of 287 °C, which remains practically lower compared with the other decomposition materials. The relatively low DTG_{max} of ANS can be explained by the amount of volatiles compared to other biomasses, which directly influence the rate of decomposition.

DTA thermogram of ANS exhibits various endothermic picks, which indicate reactions of the different components of this materiel (Fig. 4). The first peak observed at 59 °C is attributed to the energy absorbed during the evaporation of ANS. The 2nd and 3rd peaks indicate the degradation reaction of hemicellulose and cellulose respectively at 271 and 360 °C. The last peak can be attributed to the reaction of a small portion of the lignin observed at 439 °C. Generally, the decomposition of lignin takes place at a wide temperature range (200 °C to 600 °C).
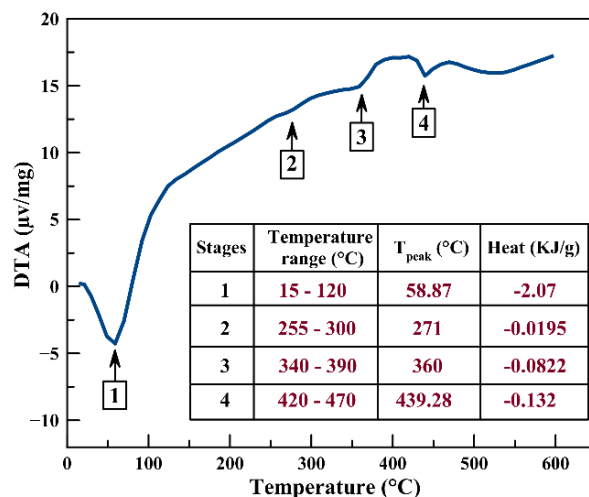

Fig. 4. DTA curve under pyrolysis condition.

3.3. Thermal behavior under oxidative atmosphere

The TG-DTG curves are shown in Fig. 5. In this case, thermal degradation process is characterized by four steps. The initial weight loss (9-10%) observed between 22 and 82 °C is attributed to the evaporation of water from ANS. The second step is observed at a temperature between 207-301°C and corresponds to the thermal degradation of the hemicellulose; this has a mass loss of 27.5 %. The third stage, at a temperature between 301-387 °C corresponds to the degradation of cellulose with a mass loss of 32.5%. The decomposition of hemicellulose and cellulose molecules mainly leads to the release of volatile matter. The last step is associated with lignin degradation between 387 and 530 °C with 29.4 % of weight loss. In general, due to its complex structure, decomposition of lignin occurs slowly in the temperature range. At the end of the oxidation, the rest of the ANS is about 1.1% (at 600 °C). Table 3 shows the TG-DTG characteristics of ANS under oxidative condition. In this case, the reactivity of ANS was found to be smaller than that founded for cotton stalk and sugar cane bagasse. This can be explained by the large T_{range} and the high T_{DTGmax} during char combustion (stage 4).
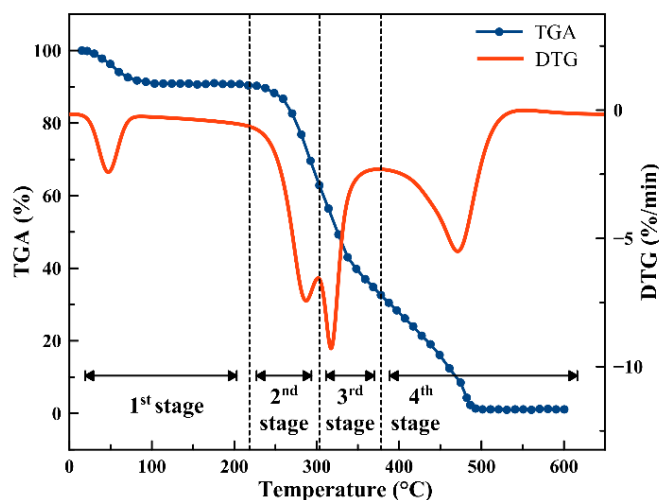
Fig. 5. TG-DTG curve under oxidative condition.

Table 3. TG-DTG characteristics of ANS under oxidative atmosphere (air) and comparison with other biomass residues.

TG-DTG characteristics		ANS	Cotton stalk	SCB
Reference		This work	[16]	[16]
Stage 2 and Stage 3	T_{range} (°C)	207-301 301-387	228-327	232-312
	$\|DTG_{max}\|$	7.38 9.23	16.8	12.6
	T_{DTGmax}	287 317	283	287
Stage 4	T_{range} (°C)	387-530	352-443	410-500
	$\|DTG_{max}\|$	5.54	7.2 0.24	4.68 8.52
	T_{DTGmax}	481	373 475	381 442
R_M*10^2		6.63	7.86	7.8

SCB: sugar cane bagasse, R_M: reactivity (% min^{-1} °C^{-1})

The DTA curve showed three thermal stages indicating physical and/or chemical reactions (Fig. 6). The endothermic peak at 55 °C is attributed to the evaporation of the water present in the particle. The first exothermic peak at a temperature of 362 °C corresponding to the decomposition of hemicelluloses and cellulose, leads to the formation and combustion of volatile products. This peak can be assimilated in the temperature range to stages 2 and 3 indicated by the TG-DTG curve in Fig. 5. The second exothermic peak at 479 °C is attributed to the total oxidation of volatiles and char part, and it is characterized by a considerable intensity compared to the first one.

DTA thermograms of ANS can also be used to determine qualitatively the heat absorbed or released by the sample during the various stages of decomposition. This is done through integrating the peak corresponding to a given transformation using the TA60 software. The DTA results are also confirmed by the TG-DTG curve and are indicated in Table 4. Thermal degradation behavior proves that

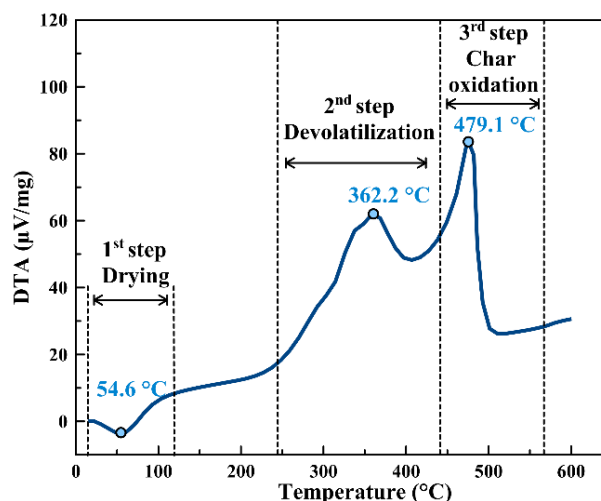combustion generates higher thermochemical conversion than pyrolysis.

Fig. 6. DTA curve under oxidative condition.

Table 4. DTA characteristics of ANS under oxidative atmosphere (air).

Characteristics	1st step	2nd step	3rd step
Nature of peak	endothermic	exothermic	exothermic
Temperature range (°C)	16 - 110	238 - 407	410 - 512
Temperature of peak (°C)	55	362	479
Heat (KJ/g)	-1.88	10.4	11.3

3.4. Kinetic parameters

To refine our study, reaction kinetic parameters like the activation energy (E_a), the frequency factor (A) and the reaction order (n) were calculated from the TG-DTG curves in pyrolytic and oxidizing condition with a heating rate of 10 °C min^{-1}. In using the independent reaction model [15, 25–27] a kinetic mechanism is proposed.

In TGA, it is customary to define the evolution of the reaction by its degree of advancement, or conversion (C):

$$C = \frac{m_0 - m}{m_0 - m_f} \tag{2}$$

Where (m_0) is the initial mass at the beginning of the step under consideration, (m_f) is the final mass of this step and (m) is the mass at any time.

The overall kinetics can be expressed, as a function of the expression of the rate, as follows:

$$-\frac{dX}{dt} = k * X^n \tag{3}$$

Where $X = 1 - C = \frac{m - m_f}{m_0 - m_f}$ is the weight of the sample (kg), n is the reaction order, k is the specific rate constant (min^{-1}), and t is the time (min). In that case, k varies with temperature according to the Arrhenius law:

$$k = A * e^{-E/RT} \qquad (4)$$

The combined equations (3) and (4) lead to the following equation:

$$-\frac{dX}{dt} = A * e^{-E/RT} * X^n \qquad (5)$$

Applying the natural logarithm operator to equation (5), it follows that:

$$ln\left(-\frac{dX}{dt}\right) = ln(A) - \frac{E}{R} * \left(\frac{1}{T}\right) + n * ln(X) \qquad (6)$$

Where $\frac{dX}{dt} = \frac{1}{m_0 - m_f} * \frac{dm}{dt}$. Replacing in (6) it follows:

$$ln\left(\frac{-1}{m_0 - m_f} * \frac{dm}{dt}\right) = ln(A) - \frac{E}{R} * \left(\frac{1}{T}\right) + n * ln\left(\frac{m - m_f}{m_0 - m_f}\right) \qquad (7)$$

This equation can be written under the form:

$$y = B + C * x + D * z \qquad (8)$$

With, $y = ln\left(\frac{-1}{m_0 - m_f} * \frac{dm}{dt}\right)$, $x = \frac{1}{T}$, $z = ln\left(\frac{m - m_f}{m_0 - m_f}\right)$, $B = ln(A)$, $C = -\frac{E}{R}$ et $D = n$

By applying the multi-linear regression technique to equation (8), the following system of equations is obtained:

$$\begin{cases} \sum_{i=1}^n y_i = nB + C \sum_{i=1}^n x_i + D \sum_{i=1}^n z_i \\ \sum_{i=1}^n x_i y_i = C \sum_{i=1}^n x_i^2 + D \sum_{i=1}^n x_i z_i + B \sum_{i=1}^n x_i \\ \sum_{i=1}^n y_i z_i = D \sum_{i=1}^n z_i^2 + C \sum_{i=1}^n x_i z_i + B \sum_{i=1}^n z_i \end{cases} \qquad (9)$$

Transform to a matrix form, and it gives:

$$\begin{pmatrix} n & \sum_{i=1}^n x_i & \sum_{i=1}^n z_i \\ \sum_{i=1}^n x_i & \sum_{i=1}^n x_i^2 & \sum_{i=1}^n x_i z_i \\ \sum_{i=1}^n z_i & \sum_{i=1}^n x_i z_i & \sum_{i=1}^n z_i^2 \end{pmatrix} * \begin{pmatrix} B \\ C \\ D \end{pmatrix} = \begin{pmatrix} \sum_{i=1}^n y_i \\ \sum_{i=1}^n x_i y_i \\ \sum_{i=1}^n y_i z_i \end{pmatrix} \qquad (10)$$

This system can be written in the linear form:

$$a * m = b \qquad (11)$$

With $m = \begin{pmatrix} B \\ C \\ D \end{pmatrix} = \begin{pmatrix} ln(A) \\ E/R \\ n \end{pmatrix} = a^{-1} * b$

The equation is solved using Matlab-R2008b software. The kinetic parameters (E_a, A, n) have been determined for devolatilization and char combustion stage as shown in Table 5.

The kinetic parameters of ANS combustion are shown to be very different than that of pyrolysis. A change from inert to oxidative atmosphere clearly results in an increase of activation energies (E) and frequency factor (A) and a decrease of peaks temperature (as indicated in table 2 and 3). It is also noted that ANS requires the least energy (58.694 KJ mol^{-1}) to get devolatilization and more energy (69.347 KJ mol^{-1}) to engender char oxidation. In addition, the frequency factor is lower during char combustion which means that this reaction occurs slowly. For ANS pyrolysis a reaction order of 0.60 is obtained in the devolatilization phase, while values on oxidative atmosphere increase (0.83) in the same phase. The coefficient of determination varies between 0.87 and 0.96, which means that the predictive power of the model is strong. This behavior is in accordance with results of El May et al. [15] and Munir et al. [16].

3.5. Combustion characteristics

3.5.1. Combustion of ANS and coal under thermogravimetric analyzer

The burning process of the ANS and charcoal was compared by TG analysis. Two samples were heated from ambient to 600 °C, with a heating rate of 10 °C min^{-1} and an air flow of 20 ml min^{-1}. Combustion parameters such as ignition and burnout temperature and their corresponding time (T_i, T_b, t_i and t_b respectively) can be evaluated from TG-DTG curves. The maximum and average mass loss rates were also evaluated. The ignition and combustion indexes (D and S, respectively) were calculated from equation (12) [28, 29].

$$D = \frac{R_{max}}{t_{max} * t_i}, \quad S = \frac{R_{max} * R_a}{T_i^2 * T_b} \qquad (12)$$

With, R_{max} (% min^{-1}) is the maximum rate of combustion in the DTG curve, t_{max} and t_i are the times corresponding to R_{max} and T_i, respectively and R_a is the average mass loss rate during combustion.

Table 5. Kinetic parameters of ANS under inert and oxidative atmospheres.

Biomass	Pyrolysis (N$_2$)				
	Temperature range (°C)	E_a (KJ mol^{-1})	A (s^{-1})	n	R^2
	231 - 415	53.75	124.04	0.602	0.88
	Oxidation (air)				
	Temperature range (°C)	E_a (KJ mol^{-1})	A (s^{-1})	n	R^2
ANS	*Devolatilization* 207 - 387	58.694	542	0.833	0.96
	Char oxidation 387 - 530	69.347	306	0.523	0.87

E: apparent activation energy; A: frequency factor; n: reaction order; R^2: coefficient of regression.

Figure. 7 illustrates the TG, DTG and DTA thermograms of coal and ANS. Overall, the coal burning process is characterized by thermal degradation over two weight losses (Fig 7a,b). The initial weight loss (7.4 %) observed between 20 and 112 °C is attributed to the evaporation of water. The second step shows the typical combustion profile between 280 and 530 °C and a maximum loss rate at 474 °C. This step is the result of volatile and char combustion. The DTG curve of the ANS (Fig. 7b) is separated into two steps (207-387 °C), reflecting the existence of different reactivity components (hemicellulose and cellulose), whereas the coal exhibits a single peak (283-522 °C), meaning it is a more homogeneous material. The coal temperature peak corresponds to the maximum loss rate in the DTG curves (474 °C) is higher than that of ANS (317 °C). Besides, the thermal degradation of ANS begins earlier at lower temperature than coal which is degraded very slowly. This is due to the difference in structure and chemical composition between ANS biomass and coal. Concerning char oxidation of ANS and coal that is represented by the last peak in DTG curves, a relatively similar DTG peak temperature of the two materials means that decomposition of ANS char is slow; this characteristic causes the low char reactivity of the material. Specifically, the greater difference between these two fuels is evident in the devolatilization phase. As illustrated in the coal TG-DTG profile (Fig. 7a, b), the combustion phase of volatiles is discrete. This result is in agreement with that found by Gaqa et al. [30]. The DTA thermogram of coal shows various peaks (Fig. 7c). The endothermic peak between 20 and 115 °C with a maximum temperature of 52 °C is attributed to the evaporation of water. The approximate heat absorbed in this step is -1.17 KJ g^{-1}. The exothermic peak observed between 154 and 528 °C has a maximum at the temperature of 475 °C. This maximum corresponding to the combustion of char produced after the devolatilization stage indicated by a shoulder at 346 °C. It is also noted that this shoulder is well confused with devolatilization phase of ANS (Fig. 7c). The combustion parameters of coal and ANS are shown in Table 6. The ignition performance of ANS is better than coal. Moreover, it burns at lower temperature and shorter time. The high reactivity of this biomass explains the high value of the combustion index. Thereby, the lower ignition and burnout temperature, the easier the fuel is combusted [29]. Finally, the released heat, estimated by DTA curve, during combustion of ANS is equal to half that of coal combustion.
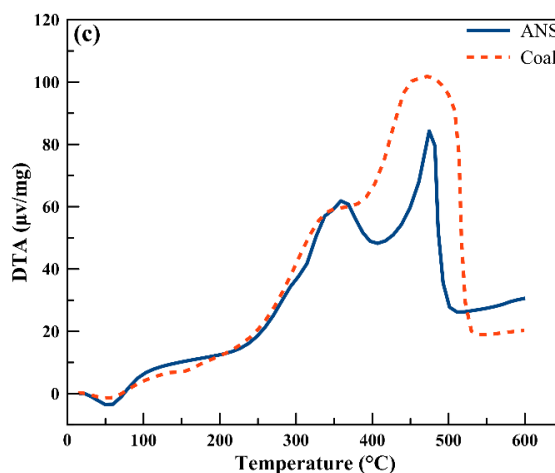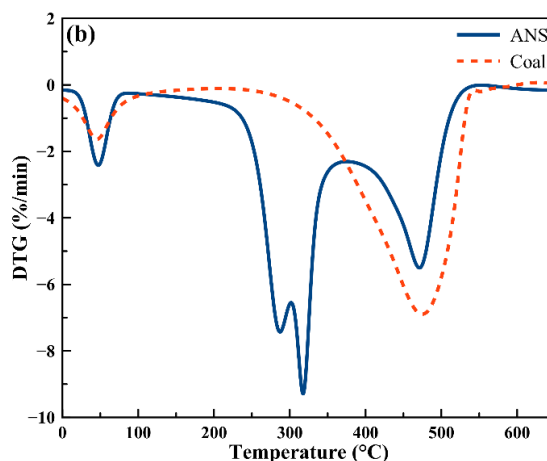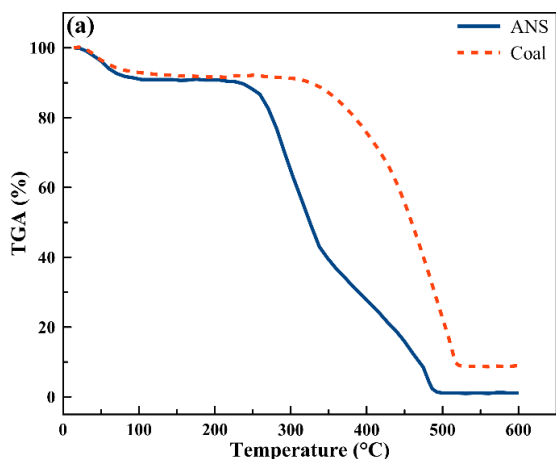

Fig. 7. TG, DTG and DTA profiles of ANS and coal: (a) TGA of ANS and coal, (b) DTG of ANS and coal, (c) DTA of ANS and coal.

Table 6. Comparison between combustion parameters of ANS and coal.

Combustion characteristics	ANS	coal
T_i (°C)	253	392
T_{max} (°C)	317.4	474.02
T_b (°C)	525.3	533
t_i (min)	23.5	36
t_b (min)	48	51.4
R_a (% min^{-1})	2.77	3.82
R_{max} (% min^{-1})	9.23	6.88
t_{max} (min)	29.23	43.2
D	0.013	0.004
$S*10^7$	7.60	3.21
DTA $_{heat}$ (KJ g^{-1})	21.7	40.5

3.5.2. Combustion behavior of single particles of ANS and coal.

Individual particles of ANS and coal was manually prepared to a cubic form to perform the combustion tests. In order to make a comparison between these fuels, the shape of the two particles and the burning conditions should be similar. The particle is placed in the reactor grid (Fig. 2) and a K-type thermocouple connected to a data logger is introduced into the center to measure the temperature up to the end of the combustion. When the heating device is switched on, the recording of the heating temperature by the data-logger and the recording of the phenomena occurring are started by a video camera. When the ignition of the particle is reached, the heating is stopped. The results obtained are shown in Fig. 8a-b. The temperature profiles of each particle were compared with the video images and each combustion phase was visible. When the ANS particle heats up (step 1), the pyrolysis begins with blackening of the surface and smoke production, followed by a period of ignition delay due to the release of the volatile material (gases). At the ignition temperature (165 °C),

there appears a yellow gas flame visible only near the solid surface (step 2). After 4 seconds of ignition, the particle is surrounded by a translucent flame (The particle is always visible.) which begins to move away from the surface, afterwards the flame is very high (almost 2.5 cm of length). Once the volatile flame is extinguished and the second stage of combustion is complete, the devolatilized particle begins to shine (step 3), indicating that char combustion is progressing (red particle). For coal particle, the appearance of the volatile flame is visible only near the solid surface and overlaps with the phase where the particle surface also begins to shine. This is due to the fact that the released volatiles cannot form a high flame in the boundary layer of the particle, and the oxygen can simply reach the solid surface. It is a hetero-homogeneous combustion that can generally be observed for pulverized coal particles [19].
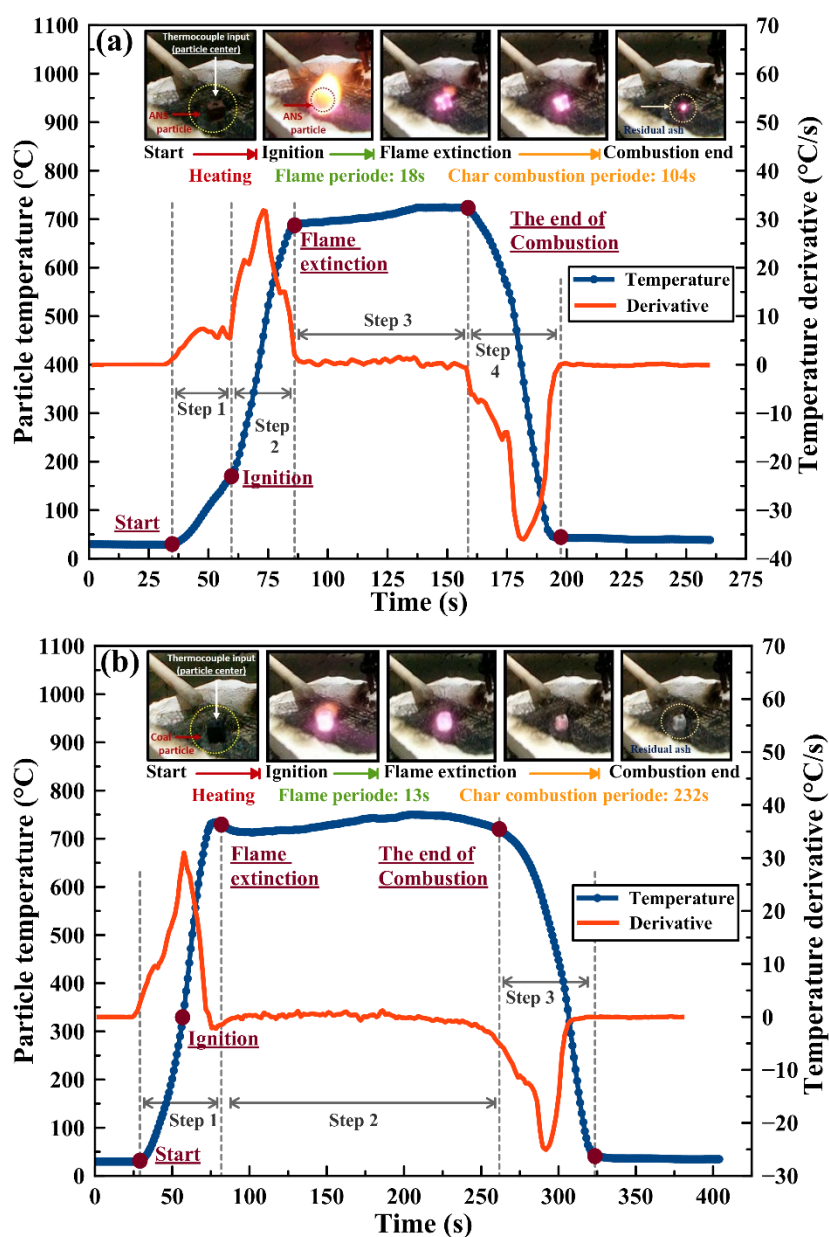

Fig. 8. Temperature profiles and sequential steps during combustion. (a) ANS particle, (b) coal particle.

Temperature of the two particles increases further, reaching a maximum value (724 and 759 °C for ANS and coal, respectively) and maintained around it for several seconds of stable char combustion. As the combustion proceeded, the particle is exhausted, its size is reduced visually until there is only a small portion of ash. At this point, the shine of the particles disappears and the temperature begins to decrease until it reaches the temperature of the environment (last step). ANS has a low ignition time and temperature with respect to the coal and a significant flame period. This can explain by the high amount of volatile matter in the ANS materials compared to coal. During the oxidation process of char, the ANS particle has a very significant lifetime and occurs up to half of coal duration.

4. Conclusion

Manufacturing of argan oil produce a significant quantity of residues that would be useful to cover energy needs. In this study, fuel properties, thermal analysis, kinetic parameters and combustion behavior of argan nut shell (ANS) biomass are studied. Physicochemical characterization results proves a heating value of 20.63 MJ kg^{-1} and negligible amount of nitrogen and sulfur. Evaluation of the thermal behaviors by TGA and DTA show very important exothermic effects. The devolatilization stage was more critical in the sample, and the significant residual char degrades slowly over a wide temperature range. During devolatilization, the calculated activation energy under both pyrolysis and oxidative atmosphere was 53.75 and 58.694 KJ mol^{-1} respectively, which are suitable for thermal energy recovery. The particle combustion has a maximum temperature of 724 °C, and the last exothermic stage has a very significant lifetime. This work allows to better understanding the thermochemical conversion of ANS, and it has been shown that this biomass should be a promising biofuel in combustion systems.

Acknowledgements

References

[1] K. E. Okedu and M. Al-hashmi, "Assessment of the cost of various renewable energy systems to provide power for a small community : case of Bukha , Oman," Int. J. Smart Grid, vol. 2, no. 3, pp. 172–182, 2018.

[2] A. Harrouz, A. Temmam, and M. Abbes, "Renewable energy in algeria and energy management systems," Int. J. Smart Grid, vol. 2, no. 1, pp. 34–39, 2018.

[3] O. T. Winarno, Y. Almendra, and S. Mujiyanto, "Policies and strategies for renewable energy developmenet in indonesia," IEEE 5th Int. Conf. Renew. Energy Res. Appl. (ICRERA), pp. 270–272, 2016.

[4] I. Carlucci, G. Mutani, and M. Martino, "Assessment of potential energy producible from agricultural biomass in the municipalities of the Novara plain," IEEE 4th Int.

Conf. Renew. Energy Res. Appl. (ICRERA), pp. 1394–1398, 2015.

[5] Y. Tosun, "Forestry biomass waste co-incineration in stoker and subsequent solar panel (CSP) ORC station," IEEE 4th Int. Conf. Renew. Energy Res. Appl. (ICRERA), pp. 583–589, 2015.

[6] A. Elorf, B. Sarh, S. Bonnamy, M. Asbik, Y. Rahib, J. Chaoufi, "Injection type effects on pulverized biomass (solid olive waste) combustion in a 50 kW combustor" Int. J. Renew. Energy Res., vol. 9, no. 2, pp. 639–648, 2019.

[7] R. E. Sims and N. El Bassam, Bioenergy Options for a Cleaner Environment, 1st ed., January. Elsevier Ltd, 2004, pp. 28-36.

[8] Z. Charrouf and D. Guillaume, "Argan oil, the 35-years-of-research product," Eur. J. Lipid Sci. Technol., vol. 116, no. 10, pp. 1316–1321, 2014.

[9] M. Zbair, M. Bottlinger, K. Ainassaari, S. Ojala, O. Stein, R. L. Keiski, M. Bensitel, R. Brahmi, "Hydrothermal carbonization of argan nut shell: functional mesoporous carbon with excellent performance in the adsorption of bisphenol A and diuron," Waste and Biomass Valorization, 2018.

[10] L. Bouqbis, S. Daoud, H.-W. Koyro, C. I. Kammann, L. F. Z. Ainlhout, and M. C. Harrouni, "Biochar from argan shells: production and characterization," Int. J. Recycl. Org. Waste Agric., vol. 5, no. 4, pp. 361–365, 2016.

[11] A. Elmouwahidi, Z. Zapata-Benabithe, F. Carrasco-Marín, and C. Moreno-Castilla, "Activated carbons from KOH-activation of argan (Argania spinosa) seed shells as supercapacitor electrodes," Bioresour. Technol., vol. 111, no. May, pp. 185–190, 2012.

[12] H. Essabir, E. Hilali, A. Elgharad, et al., "Mechanical and thermal properties of bio-composites based on polypropylene reinforced with Nut-shells of Argan particles," Mater. Des., vol. 49, pp. 442–448, 2013.

[13] Y. Rahib, B. Sarh, S. Bostyn, S. Bonnamy, T. Boushaki, and J. Chaoufi, "Non-isothermal kinetic analysis of the combustion of argan shell biomass," Mater. Today Proc., 2019.

[14] M. Alhinai, A. K. Azad, M. S. A. Bakar, and N. Phusunti, "Characterisation and Thermochemical Conversion of Rice Husk for Biochar Production," Int. J. Renew. Energy Res., vol. 8, no. 3, pp. 1648–1656, 2018.

[15] Y. El May, M. Jeguirim, S. Dorge, G. Trouvé, and R. Said, "Study on the thermal behavior of different date palm residues: Characterization and devolatilization kinetics under inert and oxidative atmospheres," Energy, vol. 44, no. 1, pp. 702–709, 2012.

[16] S. Munir, S. S. Daood, W. Nimmo, A. M. Cunliffe, and B. M. Gibbs, "Thermal analysis and devolatilization kinetics of cotton stalk, sugar cane bagasse and shea meal under nitrogen and air atmospheres," Bioresour. Technol., vol. 100, no. 3, pp. 1413–1418, 2009.

[17] E. Marek and B. Swiatkowski, "experimental studies of single particle combustion in air and different oxy-fuel atmospheres," Appl. Therm. Eng., vol. 66, pp. 35–42, 2014.

[18] J. M. Jones, A. Saddawi, B. Dooley, E. J. S. Mitchell, J. Werner and D. J. Waldron, "Low temperature ignition of biomass," Fuel Process. Technol., vol. 134, no. March, pp. 372–377, 2015.

[19] J. Riaza, J. Gibbins, and H. Chalmers, "Ignition and combustion of single particles of coal and biomass," Fuel, vol. 202, pp. 650–655, 2017.

[20] Y. Shastri, A. Hansen, L. Rodriguez, and K. C. Ting, "Engineering and science of biomass feedstock production and provision," Chapter 2, pp. 19–20, 2014.

[21] S. V Loo and J. Koppejan, The Handbook of Biomass Combustion and Co-firing, 1st ed., Earthscan, 2008, pp. 8-14.

[22] A. Elorf, N. M. Koched, T. Boushaki, B. Sarh, J. Chaoufi, S. Bostyne and I. Gokalp, "Swirl motion effects on flame dynamic of pulverized olive cake in a vertical furnace," Combust. Sci. Technol., vol. 188, no. 11–12, pp. 1951–1971, 2016.

[23] H. Essabir, "Bio-composites à base de coque de noix d'arganier: Mise en oeuvre, caractérisation et modélisation du comoportement mécanique," Ibn Zohr, 2014.

[24] A. Elabed, "Réactivité thermique et cinétique de dégradation du bois d'arganier Application à l'élaboration de charbon actif par activation chimique à l'acide phosphorique," Mohammed V – Agdal, 2007.

[25] R. S. Chutia, R. Kataki, and T. Bhaskar, "Thermogravimetric and decomposition kinetic studies of Mesua ferrea L. deoiled cake," Bioresour. Technol., vol. 139, pp. 66–72, 2013.

[26] A. Kumar, L. Wang, Y. A. Dzenis, D. D. Jones, and M. A. Hanna, "Thermogravimetric characterization of corn stover as gasification and pyrolysis feedstock," Biomass and Bioenergy, vol. 32, no. 5, pp. 460–467, 2008.

[27] F. Karaosmanoglu, B. D. Cift, and A. Isigigur-Ergudenler, "Determination of Reaction Kinetics of Straw and Stalk of Rapeseed Using Thermogravimetric Analysis," Energy Sources, vol. 23, no. 8, pp. 767–774, 2001.

[28] X. G. Li, B. G. Ma, L. Xu, Z. W. Hu, and X. G. Wang, "Thermogravimetric analysis of the co-combustion of the blends with high ash coal and waste tyres," Thermochim. Acta, vol. 441, no. 1, pp. 79–83, 2006.

[29] D. Vamvuka and S. Sfakiotakis, "Combustion behaviour of biomass fuels and their blends with lignite," Thermochim. Acta, vol. 526, no. 1–2, pp. 192–199, 2011.

[30] S. Gaqa, S. Mamphweli, D. Katwire, and E. Meyer, "The Properties and Suitability of Various Biomass/Coal Blends for Co-Gasification Purposes," J. Sustain. Bioenergy Syst., vol. 4, no. 4, pp. 175–182, 2014.